

Transfer RNA-derived fragments as novel biomarkers of the onset and progression of gastric cancer

Yaoyao Xie^{1,2} , Shuangshuang Zhang², Xiuchong Yu², Guoliang Ye^{1,3} and Junming Guo^{1,2,3}

¹Department of Biochemistry and Molecular Biology and Zhejiang Key Laboratory of Pathophysiology, School of Basic Medical Sciences, Health Science Center, Ningbo University, Ningbo 315211, China; ²Department of Gastroenterology, The First Affiliated Hospital of Ningbo University, Ningbo 315020, China; ³Institute of Digestive Diseases, Ningbo University, Ningbo 315020, China
Corresponding author: Junming Guo. Email: guojunming@nbu.edu.cn

Impact statement

The roles of transfer RNA-derived small RNAs (tsRNAs) have been investigated in various human diseases, although relatively few studies have explored the functions of tsRNAs in gastric cancer (GC). Therefore, the aim of this study was to explore the role of tRF-18-79MP9P04 (previously named tRF-5026a) in the onset and development of GC. The results of this study found that plasma levels of tRF-18-79MP9P04 were significantly decreased in early and advanced GC. High-throughput transcriptome sequencing identified genes regulated by tRF-18-79MP9P04 in GC cells, and the bioinformatics was performed to predict the functions of tRF-18-79MP9P04. Notably, tRF-18-79MP9P04 can be used as a novel non-invasive biomarker for early detection of GC and was related to cornification, the type I interferon signaling pathway, RNA polymerase II activities, and DNA binding, thereby providing a theoretical basis for further functional research and development drugs targeting tsRNAs in GC and other malignancies.

Abstract

Gastric cancer (GC) is a particularly malignant disease; thus, early diagnosis and treatment are especially important. Transfer RNA-derived small RNAs (tsRNAs) have been implicated in the onset and progression of various cancers. Therefore, the aim of this study was to explore the role of tRF-18-79MP9P04 (previously named tRF-5026a) in the onset and progression of GC. Expression levels of tRF-18-79MP9P04 were quantified in gastric mucosa specimens of healthy controls and plasma samples of patients with different stages of GC. The results showed that plasma levels of tRF-18-79MP9P04 were significantly decreased in the early and advanced stages of GC. The results of the nucleocytoplasmic separation assay found that tRF-18-79MP9P04 was localized in the nuclei of GC cells. High-throughput transcriptome sequencing identified genes regulated by tRF-18-79MP9P04 in GC cells, and the function of tRF-18-79MP9P04 was predicted by bioinformatics. Collectively, the findings of this study suggest that tRF-18-79MP9P04 would be useful as non-invasive biomarker for early diagnosis of GC and is related to cornification, the type I interferon signaling pathway, RNA polymerase II activities, and DNA binding.

Keywords: Transfer RNA-derived small RNAs, tRF-18-79MP9P04, tRF-5026a, gastric cancer, biomarker

Experimental Biology and Medicine 2023; 248: 1095–1102. DOI: 10.1177/15353702231179415

Introduction

Gastric cancer (GC) is a particularly malignant tumor and is the third most common cause of cancer-associated death worldwide.¹ According to the International Agency for Research on Cancer (IARC),² GC accounted for 1.09 million new cases and 769,000 deaths globally in 2020. The occurrence of GC is a multistage and progressive process characterized by chronic superficial gastritis, atrophic gastritis, intestinal metaplasia, and atypical hyperplasia.³ GC has no specific symptoms in the early stage. The 5-year survival rate of GC is closely associated with the disease stage at the time of diagnosis. Hence, early diagnosis and

treatment are particularly important to improve patient outcomes. Therefore, elucidation of the molecular mechanisms underlying the onset and progression of GC and identification of diagnostic biomarkers and therapeutic targets are urgently needed.

Owing to recent advancements in high-throughput RNA sequencing technology, transfer RNA-derived small RNAs (tsRNAs), which were previously described as random degradation products of transfer RNAs (tRNAs), continue to attract increasingly attention.⁴ tsRNAs, which are formed by the cleavage of mature or precursor tRNAs by specific nucleases, are classified as tRNA-derived fragments (tRFs) and tRNA halves, or tRNA-derived stress-induced RNAs

(tiRNAs), based on the cleavage site.⁵ The lengths of tRFs range from 14 to 30 nucleotides (nt) and are classified as tRF-1, tRF-2, tRF-3, tRF-5, and i-tRF. Of these, tRF-1 is a tiny fragment of 15–22 nt in length generated by cleavage of the 3' end of the precursor tRNA by RNase Z or ElaC ribonuclease Z 2,⁶ while tRF-2 is produced by cleavage of the anticodon loop, which includes the anticodon loop and stem, of the mature tRNA, but lacks the 5' and 3' ends;⁷ tRF-3 is composed of 18–22 nt derived from the 3' end of mature tRNA and is generated by cleavage of the T-loop by angiogenin (ANG), Dicer, or a member of the ribonuclease family;⁸ tRF-5, which is 14–30 nt in length, is derived from the 5' end of the mature tRNA via cleavage of the D-loop by Dicer; and i-tRF is cleaved from the internal region, including the D-loop or T-loop, of the mature tRNA, but lacks the 5' and 3' ends.^{9–11} tiRNAs are grouped into two main isoforms, known as 5' tiRNA and 3' tiRNA, derived via cleavage of the anticodon loop of the mature tRNAs by ANG.¹²

Accumulating evidence indicates that the roles of tsRNAs include regulation of gene expression, protein translation, epigenetic modifications, intercellular communication, and apoptosis.¹³ More recent studies have reported the potential of tsRNAs as cancer biomarkers. For example, plasma tRFs can distinguish between breast cancer and control, thus presenting potential novel diagnostic biomarkers.¹⁴ A previous study found that significant increase of tRF-Gln-TTG-006 level in serum acts as a novel diagnostic biomarker for hepatocellular carcinoma.¹⁵

A previous study by our group found that tRF-18-79MP9P04 (previously named tRF-5026a) suppressed the proliferation of GC cells via the PTEN/PI3K/AKT signaling pathway.¹⁶ As a continuation of our previous work, the aim of this study was to investigate the expression profiles of tRF-18-79MP9P04 as potential novel biomarkers of the onset and progression of GC and elucidate the underlying mechanisms by high-throughput transcriptome sequencing.

Materials and methods

Study approval

The study protocol was approved by the Ethics Committee of Ningbo University (approval no. 2019022501) and conducted in accordance with the ethical principles for medical research involving human subjects described in the Declaration of Helsinki. Prior to inclusion in this study, written informed consent was obtained from all subjects.

Blood sample collection

Blood samples were collected from patients with healthy gastric mucosa (HGM), benign lesions (BLs), precancerous lesions (PLs), and early gastric cancer (EGC) who were recruited from the First Affiliated Hospital of Ningbo University. Blood samples were also collected from patients with advanced gastric cancer (AGC) who were recruited from the First Affiliated Hospital of Ningbo University. All subjects underwent gastroscopic examinations. Histopathological diagnoses were made by an experienced pathologist.

Cell culture

Normal gastric mucosa epithelial GES-1 cells were obtained from the Beijing Beina Chuanglian Institute of Biotechnology (Beijing China). Gastric adenocarcinoma AGS and metastatic GC HGC-27 cells were acquired from the Cell Resource Center of the Shanghai Institutes for Biological Sciences (Chinese Academy of Sciences, Shanghai, China). The GES-1 and AGS cells were cultured in high-glucose Dulbecco's modified Eagle's medium supplemented with 10% fetal bovine serum and 1% penicillin/streptomycin. HGC-27 cells were cultured in Roswell Park Memorial Institute 1640 medium supplemented with 10% fetal bovine serum and 1% penicillin/streptomycin. All cells were incubated at 37°C under an atmosphere of 5% CO₂/95% air.

RNA extraction and quality testing

Total RNA was extracted from cells and plasma samples with TRIzol and TRIzol LS reagents, respectively (Thermo Fisher Scientific, Waltham, MA, USA) in accordance with the manufacturer's instructions. Nucleoplasmic RNA was extracted using the PARISTM Kit Protein and RNA Isolation System kit (Invitrogen Corporation, Carlsbad, CA, USA). The concentration and purity of the RNA were determined with a spectrophotometer (DeNovix Inc., Wilmington, DE, USA). The RNA was considered sufficiently pure at an A_{260}/A_{280} ratio of 1.8–2.1. The RNA was stored at –80°C for later use.

Reverse transcription of RNA

Total RNA was reverse transcribed into complementary DNA (cDNA) using the Tiosbio™ Polestar 1st cDNA Synthesis Kit (gDNA removal) (Tiosbio, Beijing, China).

Quantitative reverse transcription polymerase chain reaction

Cellular expression of tRF-18-79MP9P04 was quantified by quantitative reverse transcription-polymerase chain reaction (qRT-PCR) using the SYBR dye method with U6 small nuclear RNA as an internal reference and performed with KOD SYBR® quantitative polymerase chain reaction (qPCR) Mix (Toyobo, Osaka, Japan) and a QuantStudio™ 3 Real-Time PCR System (Thermo Fisher Scientific).

Plasma expression levels of tRF-18-79MP9P04 were quantified by absolute fluorescence qRT-PCR using the TaqMan dye method with a specific hydrolysis probe complementary to the template designed to enhance the specificity of detection. A recombinant pUC57 plasmid coding for tRF-18-79MP9P04 was constructed by General Biosystems (Anhui) Co., Ltd. (Anhui, China). The concentration and purity of the recombinant plasmid DNA were measured with a spectrophotometer (DeNovix Inc.). The copy number of the recombinant plasmid was calculated with the formula: copy number = plasmid concentration \times 6.02 \times 10²³ / (660 \times total length of the plasmid). Then, the plasmid was diluted with RNase-free water to 1 \times 10⁷ copies/ μ L as the stock solution, which was serially diluted by 10-fold (1 \times 10⁶, 1 \times 10⁵, 1 \times 10⁴, 1 \times 10³, 1 \times 10², and 1 \times 10 copies/ μ L) with RNase-free water. The plasmid dilutions were used as the amplification templates for construction of a standard curve.

Amplifications were performed with TOROIVD® 5G qPCR Premix (Toroivd, Shanghai, China) with the diluted plasmids or cDNA as the amplification template with a QuantStudio™ 3 Real-Time PCR System. All primers (Supplemental Table 1) were constructed by General Biosystems (Anhui) Co., Ltd.

High-throughput sequencing

Total RNA was extracted from AGS cells transfected with the tRF-18-79MP9P04 mimics or negative control (NC). High-throughput transcriptome sequencing was performed by Shanghai OE Biotech Co., Ltd. (Shanghai, China). Gene ontology (GO) enrichment analysis of the differentially expressed genes (DEGs) was performed with reference to the Kyoto Encyclopedia of Genes and Genomes (KEGG) database. The Database for Annotation, Visualization and Integrated Discovery (<https://david.ncifcrf.gov/>) was used to explore the biological function of tRF-18-79MP9P04.

Statistical analysis

Statistical analyses were conducted with IBM SPSS Statistics for Windows, version 21.0. (IBM Corporation, Armonk, NY, USA). The figures were generated using GraphPad Prism 7 (GraphPad Software Inc., San Diego, CA, USA) and Adobe Photoshop CC 2017 (Adobe, Inc., San Jose, CA, USA). Data comparisons were performed using the Mann–Whitney *U* test or the Kruskal–Wallis *H* test, where appropriate. Non-normally distributed data are presented as the median and interquartile range. A probability (*P*) value < 0.05 was considered statistically significant.

Results

Characteristics and amplification results of tRF-18-79MP9P04

Queries of the MINTbase database (<https://cm.jefferson.edu/MINTbase/>) revealed that the length of tRF-18-79MP9P04 is 18 nt and derived from the 5' ends of tRNA-Val-AAC and tRNA-Val-CAC (76 nt), which matched the 5' ends of 18 human tRNAs, and the cleavage site was located in the D ring (Supplemental Figure 1). The base sequence of tRF-18-79MP9P04 is 5'-GUUUCGUAUGUGUAGUGG-3', which is the same as that of tRF-5026a, in agreement with the results of our previous study.¹⁶ Based on the sequence of tRF-18-79MP9P04, specific reverse transcription, upstream, and downstream primers were designed (Supplemental Table 1) to quantify the expression levels of tRF-18-79MP9P04 by qRT-PCR. The length of the qRT-PCR product was 73 bp. The position of the qRT-PCR product band of tRF-18-79MP9P04 was consistent with the theoretical position by agarose gel electrophoresis (Figure 1). The sequence of the qRT-PCR product, as determined with the TA Cloning® Kit (Thermo Fisher Scientific), was consistent with the sequence retrieved from the MINTbase database (Supplemental Figure 2).

Plasma levels of tRF-18-79MP9P04 in GC-related processes

Since that there is no ideal reference for quantification of tsRNAs level in bodily fluids, a method to quantify plasma

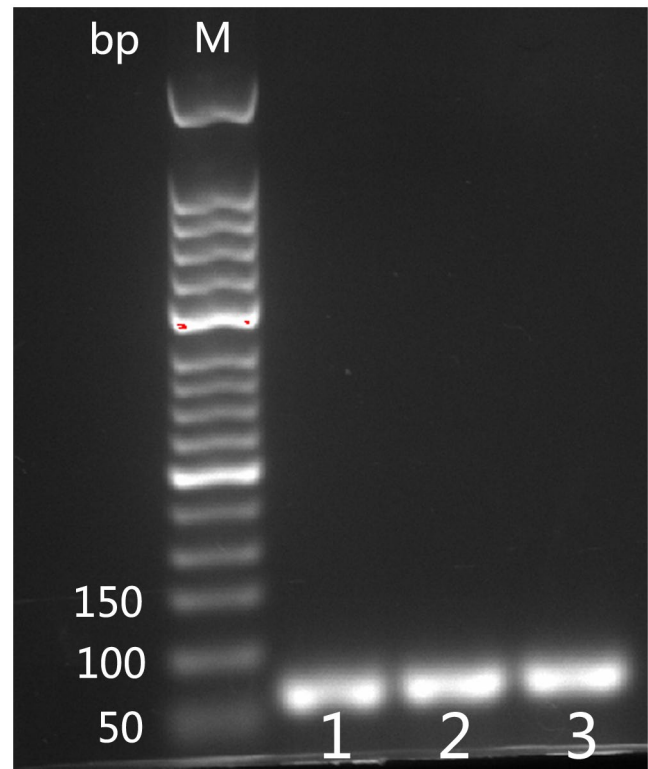


Figure 1. Electrophoresis results of qRT-PCR products.

levels of tRF-18-79MP9P04 was established. Briefly, the cDNA amplification product of tRF-18-79MP9P04 was cloned into the pUC57 plasmid by General Biosystems (Anhui) Co., Ltd. (Supplemental Figure 3).

For detection of tRF-18-79MP9P04 in plasma samples by qRT-PCR, the recombinant plasmids were serially diluted to obtain the C_q value. The formula of the standard curve was $y = -3.590x + 43.910$ with a coefficient of determination $R^2 = 0.999$ (Supplemental Figure 4), thus indicating that the established standard curve can accurately reflect amplification of tRF-18-79MP9P04.

Comparisons of the plasma levels of tRF-18-79MP9P04 among the HGM, BL, PL, EGC, and AGC groups found significant decreases in the copy number of tRF-18-79MP9P04 in the EGC and AGC groups, but no significant difference between the BL and PL groups (Figure 2(A)). A heatmap of the $-\log_{10}$ changes to the *P* values showed that the largest difference in the copy number of tRF-18-79MP9P04 was between the HGM and AGC groups (Figure 2(B)).

Diagnostic value of plasma levels of tRF-18-79MP9P04

Analysis of the diagnostic value of tRF-18-79MP9P04 in the plasma samples of the HGM, BL, PL, EGC, and AGC groups (Table 1) found that the largest area under the receiver operator characteristic curve (AUC) of 0.736 occurred between the BL and EGC groups (Figure 3), while the sensitivity and specificity were 0.431 and 0.958, respectively, the positive predictive value was 0.939, and the negative predictive value was 0.529.

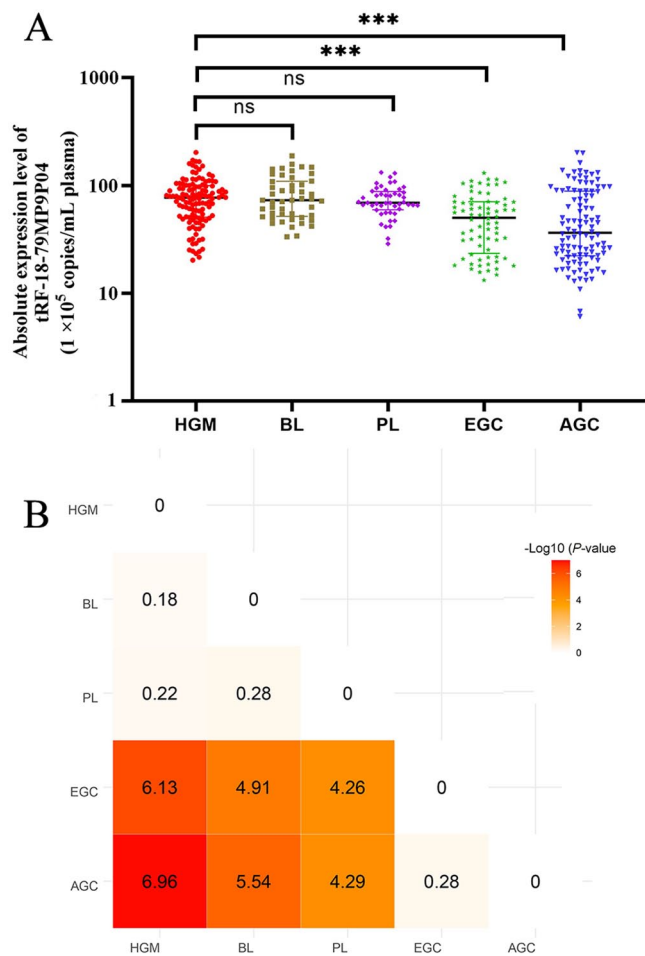


Figure 2. Plasma levels of tRF-18-79MP9P04 in GC-related processes. (A) Plasma levels of tRF-18-79MP9P04 in GC-related processes. (B) Comparison of data among groups. A heatmap of the $-\log_{10}$ changes to the P values. HGM: healthy gastric mucosa ($n=120$); BL: benign lesion ($n=48$); PL: precancerous lesion ($n=48$); EGC: early gastric cancer ($n=72$); AGC: advanced ($n=108$); ns: no significance. *** $P < 0.001$.

Nucleocytoplasmic localization of tRF-18-79MP9P04

To elucidate the biological function of tRF-18-79MP9P04, the localization of tRF-18-79MP9P04 in GES-1, AGS, and HGC-27 cells was determined with the nucleocytoplasmic separation assay with U6 small nuclear RNA (snRNA) and glyceraldehyde 3-phosphate dehydrogenase (GAPDH) mRNA as nuclear and cytoplasmic markers, respectively. The results showed that the RNAs were successfully isolated from the nucleocytoplasm (Figure 4). The results of the nucleocytoplasmic separation assay showed that tRF-18-79MP9P04 was mainly localized in the nucleus (Figure 4).

Results of high-throughput transcriptome sequencing

The total RNA extracted from AGS cells transfected with tRF-18-79MP9P04 mimics or the NC was applied for high-throughput transcriptome sequencing. Screening of the mRNAs based on an adjusted P value < 0.05 and fold change

> 2 identified 56 DEGs between the tRF-18-79MP9P04 mimics and NC groups (Figure 5). The functions of the mRNAs, as determined by GO enrichment analysis based on the KEGG database, were categorized as biological processes (BPs), cellular components (CCs), or molecular functions (MFs). The enriched BPs of the DEGs included "cornification", "type I interferon signaling pathway", "sodium ion transmembrane transport", and "viral process," while the enriched CCs included "integral component of endoplasmic reticulum membrane" and "extracellular exosome," and the enriched MFs included "RNA polymerase II cis-regulatory region sequence-specific DNA binding", "actin filament binding", "DNA-binding transcription factor activity", "RNA polymerase II-specific", "herpes simplex virus 1 infection", and "adrenergic signaling in cardiomyocytes" (Table 2).

The KEGG enrichment results showed that tRF-18-79MP9P04 was mainly associated with "herpes simplex virus type I infection" and "adrenergic signaling in cardiomyocytes" (Table 3).

Discussion

The onset and progression of GC pose severe threats to human health. Despite the continued improvement in diagnosis and treatment strategies, the morbidity and mortality rates of GC remain high.¹⁷ A large proportion of deaths due to GC are attributable to delayed diagnosis and treatment. However, treatment options are limited for patients diagnosed with advanced or metastatic GC. Thus, highly sensitive and specific biomarkers for early detection of GC are urgently needed.

High-throughput RNA sequencing technology has facilitated the identification of novel non-coding small RNAs, including tsRNAs, as diagnostic biomarkers for cancers of the breast, colon, rectum, and stomach.^{18–22} A previous study by our group found that tRF-5026a (tRF-18-79MP9P04) acts as a tumor suppressor in GC through the PTEN/PI3K/AKT signaling pathway.¹⁶ As a continuation of this work, the results of this study determined that tRF-18-79MP9P04 was an 18-nt segment derived from the 5' ends of tRNA-Val-AAC and tRNA-Val-CAC, belonging to the tRF-5 subgroup. Hu *et al.*²³ reported that upregulation of tRF-5 was associated with an increased risk of postoperative recurrence and poor prognosis of lung adenocarcinoma, demonstrating that tRFs present in bodily fluids (e.g. plasma, serum, and urine) are potential non-invasive biomarkers for the diagnosis of malignancies.

The development of GC is a multistage process; thus, the expression profiles of tRF-18-79MP9P04 were investigated in plasma samples collected from five patient groups (HGM, BL, PL, EGC, and AGC) to determine whether tRF-18-79MP9P04 is involved in the onset and progression of GC. The results showed that as compared to healthy controls (HGM group), the copy number of tRF-18-79MP9P04 was significantly decreased in the EGC and AGC groups (Figure 2), while the largest AUCs were between the BL and EGC groups (AUC=0.736) and between the BL and AGC groups (AUC=0.735) (Table 1), demonstrating that plasma tRF-18-79MP9P04 can be used to identify the onset and progression of GC.

Table 1. Diagnostic value of plasma tRF-18-79MP9P04 in gastric cancer-related processes.

Groups	AUC	Sensitivity	Specificity	Cut-off (copies/mL)	PPV	NPV
HGM versus BL	0.522	0.229	0.892	11,809,322	0.458	0.743
HGM versus PL	0.526	0.854	0.283	9,704,711	0.323	0.829
HGM versus EGC	0.714	0.681	0.667	6,275,240	0.551	0.777
HGM versus AGC	0.704	0.611	0.808	4,774,077	0.742	0.698
BL versus PL	0.537	0.875	0.313	9,950,057	0.560	0.714
BL versus EGC	0.736	0.431	0.958	4,069,975	0.939	0.529
BL versus AGC	0.735	0.528	0.958	4,007,097	0.966	0.474
PL versus EGC	0.718	0.681	0.723	6,358,212	0.790	0.603
PL versus AGC	0.704	0.546	0.958	4,131,580	0.967	0.484
EGC versus AGC	0.528	0.435	0.722	3,083,032	0.701	0.460

HGM: healthy gastric mucosa; BL: benign lesion; PL: precancerous lesion; EGC: early gastric cancer; AGC: advanced gastric cancer; AUC: area under curve; PPV: positive predictive value; NPV: negative predictive value.

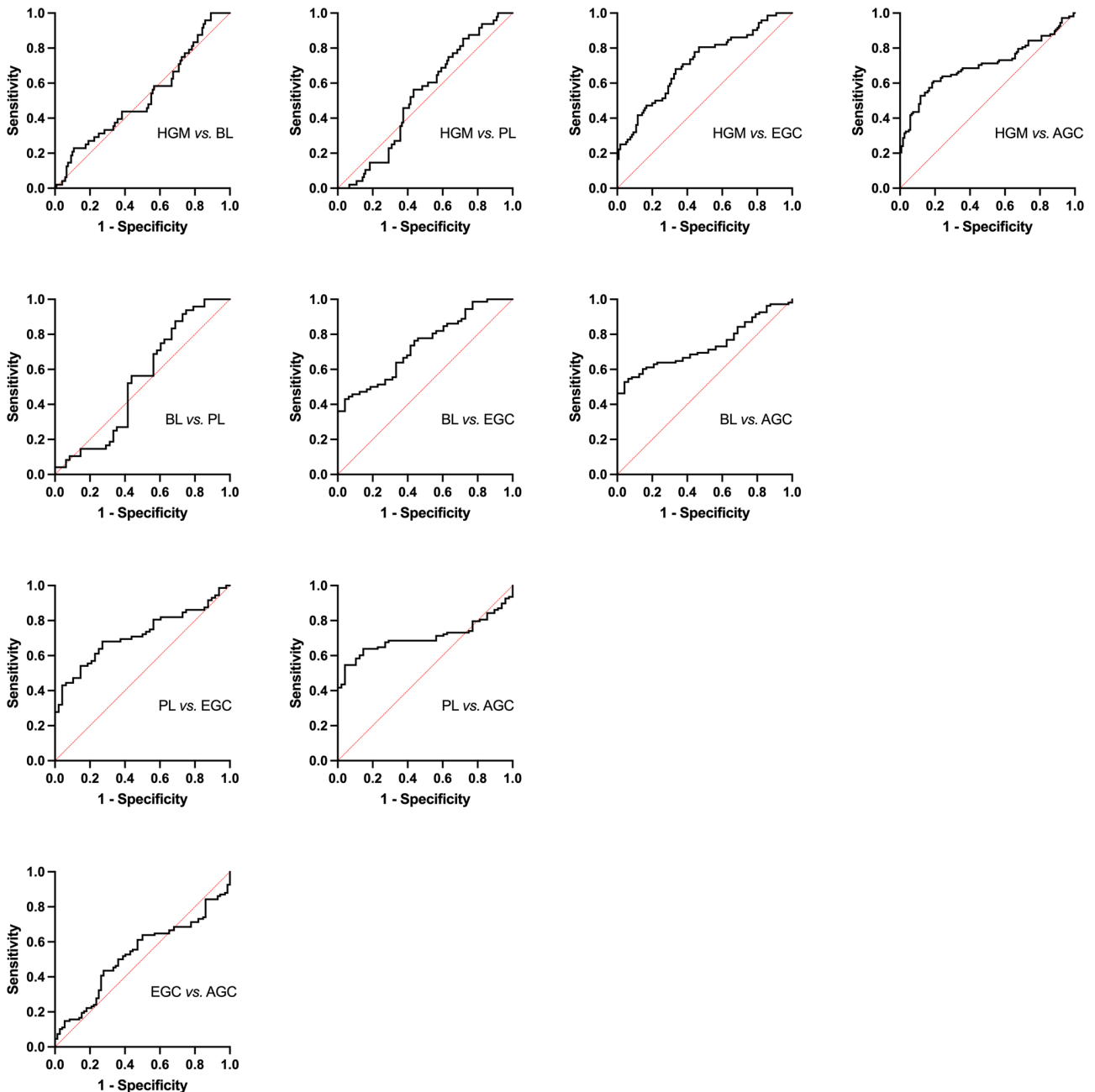


Figure 3. AUC of plasma tRF-18-79MP9P04 related to the progression of GC. HGM: healthy gastric mucosa; BL: benign lesion; PL: precancerous lesion; EGC: early gastric cancer; AGC: advanced gastric cancer; AUC: area under curve.

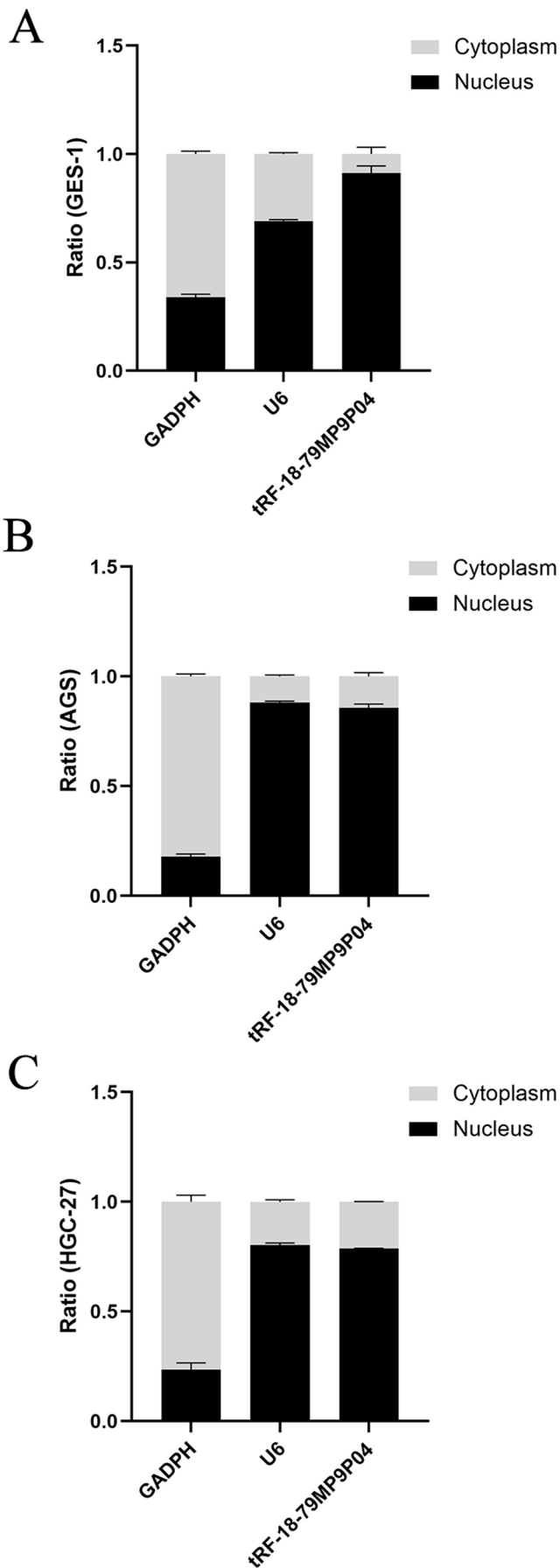


Figure 4. Nucleocytoplasmic localization of tRF-18-79MP9P04 in (A) GES-1, (B) AGS, and (C) HGC-27 cells ($n=3$).

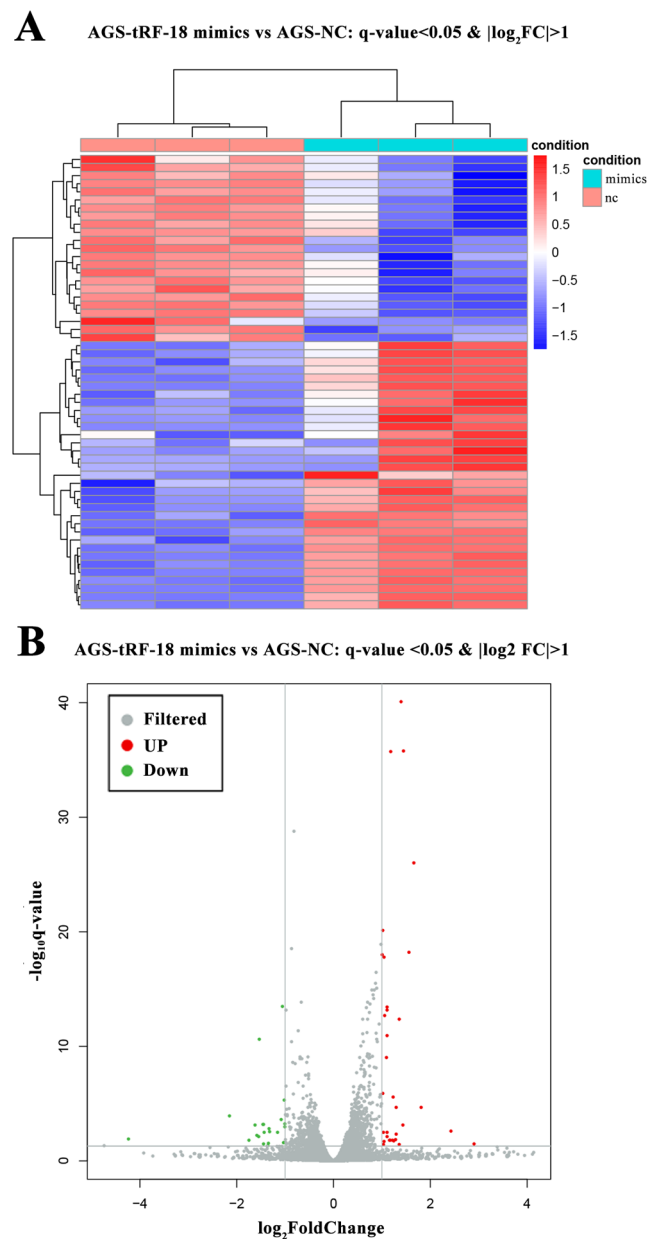


Figure 5. High-throughput transcriptome sequencing results of GC cells treated with tRF-18-79MP9P04 mimics. (A) Hierarchical clustering heatmap. Each row represents an mRNA and each column represents a sample. (B) A volcano plot of the two groups.

Early detection of GC is critical to improve patient outcomes. Plasma tRFs present promising novel diagnostic biomarkers for breast cancer²⁴ as well as other malignancies.⁶⁻⁸ A study conducted by Zhang *et al.*²² found that tRF-Gly-CCC-046, tRF-Tyr-GTA-010, and tRF-Pro-TGG-001 combined with some traditional biomarkers could be used to effectively monitor the progression of breast cancer. At present, diagnosis of GC is mainly based on endoscopic and histopathological examinations of lesions and a differential diagnosis is usually required to distinguish primary GC from other diseases. Although there have been relatively few studies, tsRNAs are reportedly effective for screening and diagnosis of early GC and to select effective and reliable treatment strategies. The results of a previous study by our group found that serum level of tRF-5026a (tRF-18-79MP9P04) was correlated

Table 2. GO analysis of tRF-18-79MP9P04 upregulated genes.

Category	Term	Genes	P value
GO_BP_DIRECT	Cornification	<i>KRT6A, KRT6B, PERP, SPRR2D</i>	<0.001
GO_BP_DIRECT	Type I interferon signaling pathway	<i>IFIT1, RSAD2, XAF1</i>	0.001
GO_BP_DIRECT	Sodium ion transmembrane transport	<i>SCN1B, SLC17A7, SLC34A3</i>	0.003
GO_BP_DIRECT	Viral process	<i>G3BP2, IFIT1, PRMT6, PSMB9, RSAD2</i>	0.012
GO_CC_DIRECT	Integral component of endoplasmic reticulum membrane	<i>DHRS9, EMC6, PORCN</i>	0.005
GO_CC_DIRECT	Extracellular exosome	<i>CD22, CFL2, H2BC5, KRT6A, KRT6B, LCP1, ORM2, PSMB9, S100P, STOM, TPM4</i>	0.040
GO_MF_DIRECT	RNA polymerase II cis-regulatory region sequence-specific DNA binding	<i>FOSB, ZNF354A, ZNF468, ZNF492, ZNF616, ZNF630, ZNF678, ZNF765</i>	0.021
GO_MF_DIRECT	Actin filament binding	<i>CFL2, LCP1, TPM4</i>	0.024
GO_MF_DIRECT	DNA-binding transcription factor activity, RNA polymerase II-specific	<i>FOSB, ZNF354A, ZNF468, ZNF492, ZNF616, ZNF630, ZNF678, ZNF765</i>	0.028

Table 3. KEGG analysis of tRF-18-79MP9P04 upregulated genes.

Category	Term	Genes	P value
KEGG_PATHWAY	Herpes simplex virus 1 infection	<i>ZNF354A, ZNF468, ZNF492, ZNF616, ZNF630, ZNF765</i>	0.007
KEGG_PATHWAY	Adrenergic signaling in cardiomyocytes	<i>RYR2, TPM4, SCN1B</i>	0.016

with serum level of the tumor marker carbohydrate antigen 19-9 and tumor size, indicating that tRF-18-79MP9P04 is a potential novel diagnostic biomarker for GC.¹⁶ Meanwhile, the results of this study found that plasma tRF-18-79MP9P04 was a useful biomarker for early detection of GC (Figure 3).

Further analysis clarified that tRF-18-79MP9P04 was mainly localized in the nucleus (Figure 4). Through high-throughput transcriptome sequencing of differentially expressed mRNAs after tRF-18-79MP9P04 was over-expressed in GC cells, we performed GO and KEGG enrichment analyses and found that in terms of BP, tRF-18-79MP9P04 was mainly enriched in cornification and others (Tables 2 and 3). GO enrichment analysis found that tRF-18-79MP9P04 was involved in the onset and progression of GC (Table 2). Werner *et al.*²⁵ found that the use of cornification and keratins as diagnostic biomarkers of various cancers, especially tumor cell dissemination, metastasis, and treatment responsiveness. In fact, a study by Xiong *et al.*²⁶ found that lung adenocarcinoma was associated with cornification.

GO enrichment analysis found that the DEGs identified in this study were involved in the immune response, including the type I interferon signaling pathway (Table 2), suggesting that the immune response is closely related to the progression of GC. The type I interferon signaling pathway can directly or indirectly regulate tumor growth by acting on tumor cells and immune cells, respectively.²⁷ Changes to the expression levels of tRF-18-79MP9P04 were linked to mRNA levels of X-linked inhibitor of apoptosis-associated factor 1 (XAF1). Zhang *et al.*²⁸ found that expression of XAF1 in GC is negatively correlated to the p53 tumor suppressor protein, which can inhibit the transcription of XAF1 by interacting with high-affinity response elements (−95 to −86nt) within the XAF1 promoter, indicating a potential relationship among tRF-18-79MP9P04, p53, and XAF1.

GO enrichment analysis also identified DEGs involved in RNA polymerase II activities and DNA binding (Table 2). These findings indicate that tRF-18-79MP9P04 also plays important

roles in various cellular processes that could be linked to the onset and progression of GC.

Several recent studies have investigated the use of tsRNAs as potential therapeutic targets.^{7,8,10,22} The results of our previous study established the impact of tRF-18-79MP9P04 in the onset and progression of GC via the PTEN/PI3K/AKT signaling pathway,¹⁶ while the findings of this study implicated tRF-18-79MP9P04 in cornification, the type I interferon signaling pathway, RNA polymerase II activities, and DNA binding (Tables 2 and 3), thereby presenting promising future directions of research to elucidate the mechanisms employed by tsRNA in the development of GC.

Conclusions

The results of this study confirmed that tRF-18-79MP9P04 presents a novel non-invasive biomarker for early diagnosis of GC. In addition, the involvement of tRF-18 in cornification, the type I interferon signaling pathway, RNA polymerase II activities, and DNA binding provide a theoretical basis for further functional research and development of drugs targeting tsRNAs.

AUTHORS' CONTRIBUTIONS

JG designed the study. YX and JG wrote the manuscript. XY, SZ, YX, and GY collected the clinical information. All of the authors participated in revisions of the manuscript and approved the final version for publication.

DECLARATION OF CONFLICTING INTERESTS

The author(s) declared no potential conflicts of interest with respect to the research, authorship, and/or publication of this article.

ETHICAL APPROVAL

The study protocol was approved by the Ethics Committee of Ningbo University (approval no. 2019022501) and conducted

in accordance with the ethical principles for medical research involving human subjects described in the Declaration of Helsinki. Prior to inclusion in this study, written informed consent was obtained from all subjects.

FUNDING

The author(s) disclosed receipt of the following financial support for the research, authorship, and/or publication of this article: This study was financially supported by grants from the National Natural Science Foundation of China (no. 81974316), the Zhejiang Provincial Natural Science Foundation of China (no. LGF21H200004), the Ningbo Municipal Bureau of Science and Technology (nos 2021Z133 and 2022Z130), the Medical and Health Science and Technology Project of Zhejiang Province (no. 2022RC064), and the K.C. Wong Magna Fund of Ningbo University.

ORCID ID

Yaoyao Xie  <https://orcid.org/0000-0001-7336-2385>

SUPPLEMENTAL MATERIAL

Supplemental material for this article is available online.

REFERENCES

- Sung H, Ferlay J, Siegel R, Laversanne M, Soerjomataram I, Jemal A, Bray F. Global cancer statistics 2020: GLOBOCAN estimates of incidence and mortality worldwide for 36 cancers in 185 countries. *CA Cancer J Clin* 2021;**71**:209–49
- International Agency for Research on Cancer (IARC), <https://www.iarc.who.int/>
- Correa P, Haenszel W, Cuello C, Tannenbaum S, Archer M. A model for gastric cancer epidemiology. *Lancet* 1975;**2**:58–60
- Kumar P, Anaya J, Mudunuri S, Dutta A. Meta-analysis of tRNA derived RNA fragments reveals that they are evolutionarily conserved and associate with AGO proteins to recognize specific RNA targets. *BMC Biol* 2014;**12**:78
- Liu B, Cao J, Wang X, Guo C, Liu Y, Wang T. Deciphering the tRNA-derived small RNAs: origin, development, and future. *Cell Death Discov* 2021;**13**:24
- Xie Y, Yao L, Yu X, Ruan Y, Li Z, Guo J. Action mechanisms and research methods of tRNA-derived small RNAs. *Signal Transduct Target Ther* 2020;**5**:109
- Qin C, Xu P, Zhang X, Zhang C, Liu C, Yang D, Gao F, Yang M, Du L, Li J. Pathological significance of tRNA-derived small RNAs in neurological disorders. *Neural Regen Res* 2020;**15**:212–21
- Zhu L, Ge J, Li T, Shen Y, Guo J. tRNA-derived fragments and tRNA halves: the new players in cancers. *Cancer Lett* 2019;**452**:31–7
- Yu X, Xie Y, Zhang S, Song X, Xiao B, Yan Z. tRNA-derived fragments: mechanisms underlying their regulation of gene expression and potential applications as therapeutic targets in cancers and virus infections. *Theranostics* 2021;**11**:461–9
- Kim H. Transfer RNA-derived small non-coding RNA: dual regulator of protein synthesis. *Mol Cells* 2019;**42**:687–92
- Park E, Kim T. Fine-tuning of gene expression by tRNA-derived fragments during abiotic stress signal transduction. *Int J Mol Sci* 2018;**19**:518
- Wen J, Huang Z, Li Q, Chen X, Qin H, Zhao Y. Research progress on the tsRNA classification, function, and application in gynecological malignant tumors. *Cell Death Discov* 2021;**7**:388
- Perona B, Bartolome J, Sepka R, Serafin D, Klitzman B. Acute difluoromethylornithine treatment increases skin flap survival in rats. *Ann Plast Surg* 1990;**25**:26–8
- Wang J, Ma G, Ge H, Han X, Mao X, Wang X, Veeramootoo J, Xia T, Liu X, Wang S. Circulating tRNA-derived small RNAs (tsRNAs) signature for the diagnosis and prognosis of breast cancer. *NPJ Breast Cancer* 2021;**7**:4
- Zhan S, Yang P, Zhou S, Xu Y, Xu R, Liang G, Zhang C, Chen X, Yang L, Jin F, Wang Y. Serum mitochondrial tsRNA serves as a novel biomarker for hepatocarcinoma diagnosis. *Front Med* 2022;**16**:216–26
- Zhu L, Li Z, Yu X, Ruan Y, Shen Y, Shao Y, Zhang X, Ye G, Guo J. The tRNA-derived fragment 5026a inhibits the proliferation of gastric cancer cells by regulating the PTEN/PI3K/AKT signaling pathway. *Stem Cell Res Ther* 2021;**12**:418
- Cao M, Li H, Sun D, He S, Lei L, Peng J, Chen W. Epidemiological trend analysis of gastric cancer in China from 2000 to 2019. *Chin J Dig Surg* 2021;**20**:102–9
- Huang S, Sun B, Xiong Z, Shu Y, Zhou H, Zhang W, Xiong J, Li Q. The dysregulation of tRNAs and tRNA derivatives in cancer. *J Exp Clin Cancer Res* 2018;**37**:101
- Rashad S, Niizuma K, Tominaga T. tRNA cleavage: a new insight. *Neural Regen Res* 2020;**15**:47–52
- Pandey K, Madhry D, Ravi Kumar Y, Malvankar S, Sapra L, Srivastava R, Bhattacharyya S, Verma B. Regulatory roles of tRNA-derived RNA fragments in human pathophysiology. *Mol Ther Nucleic Acids* 2021;**26**:161–73
- Yang H, Zhang H, Chen Z, Wang Y, Gao B. Effects of tRNA-derived fragments and microRNAs regulatory network on pancreatic acinar intracellular trypsinogen activation. *Bioengineered* 2022;**13**:3207–20
- Zhang Y, Bi Z, Dong X, Yu M, Wang K, Song X, Xie L, Song X. tRNA-derived fragments: tRF-Gly-CCC-046, tRF-Tyr-GTA-010 and tRF-Pro-TGG-001 as novel diagnostic biomarkers for breast cancer. *Thorac Cancer* 2021;**12**:2314–23
- Hu F, Niu Y, Mao X, Cui J, Wu X, Simone C, Kang H, Qin W, Jiang L. tsRNA-5001a promotes proliferation of lung adenocarcinoma cells and is associated with postoperative recurrence in lung adenocarcinoma patients. *Transl Lung Cancer Res* 2021;**10**:3957–72
- Wang J, Ma G, Li M, Han X, Xu J, Liang M, Mao X, Chen X, Xia T, Liu X, Wang S. Plasma tRNA fragments derived from 5' ends as novel diagnostic biomarkers for early-stage breast cancer. *Mol Ther Nucleic Acids* 2020;**21**:954–64
- Werner S, Keller L, Pantel K. Epithelial keratins: biology and implications as diagnostic markers for liquid biopsies. *Mol Aspects Med* 2020;**72**:100817
- Xiong Y, Feng Y, Qiao T, Han Y. Identifying prognostic biomarkers of non-small cell lung cancer by transcriptome analysis. *Cancer Biomark* 2020;**27**:243–50
- Yu R, Zhu B, Chen D. Type I interferon-mediated tumor immunity and its role in immunotherapy. *Cell Mol Life Sci* 2022;**79**:191
- Zhang W, Guo Z, Jiang B, Niu L, Xia G, Wang X, Cheng T, Zhang Y, Wang J. Identification of a functional p53 responsive element within the promoter of XAF1 gene in gastrointestinal cancer cells. *Int J Oncol* 2010;**36**:1031–7

(Received December 14, 2022, Accepted February 27, 2023)